

UC Davis

UC Davis Previously Published Works

Title

Experimental estimates of compression heating and decompression cooling in ethylene glycol.

Permalink

<https://escholarship.org/uc/item/3x75c63p>

Journal

Magnetic Resonance in Chemistry, 58(2)

Authors

Steele, J
Augustine, Matthew
Ames, James

Publication Date

2020-02-01

DOI

10.1002/mrc.4961

Peer reviewed



Published in final edited form as:

Magn Reson Chem. 2020 February ; 58(2): 163–169. doi:10.1002/mrc.4961.

Experimental Estimates of Compression Heating and Decompression Cooling in Ethylene Glycol

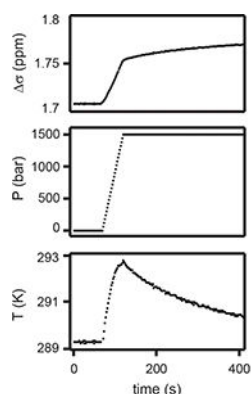
J. Steele, J. Ames, M. P. Augustine^{a)}

Department of Chemistry, One Shields Avenue, University of California, Davis, CA 95616

Abstract

The chemical shift difference, σ , between the methylene and hydroxyl protons in the high resolution ^1H nuclear magnetic resonance spectrum of ethylene glycol is shown to be pressure dependent. The equilibrium σ values for ethylene glycol are reported as a function of temperature and pressure between ambient conditions, 323 K, and 2 kbar respectively. This surface is used along with σ values measured in response to a rapid pressure increase to calculate a temperature rise that is used to infer a temperature change for water that is consistent with theoretical estimates. This work implies that compression heating and decompression cooling are not significant enough to interfere with pressure induced protein folding studies.

Graphical Abstract



The well known temperature dependent ^1H chemical shift difference $\Delta\sigma$ between the hydroxyl and methylene protons in ethylene glycol is shown to also be pressure dependent. A $\Delta\sigma$ surface as a function of temperature and pressure is constructed and used to experimentally determine the temperature rise during sample compression and recovery as equilibrium is established at elevated pressure. This work suggests that temperature changes during sample compression and decompression are not significant enough to interfere with protein folding studies.

Keywords

NMR; ^1H ; pressure standard; compression heating; decompression cooling

1.0 Introduction

The folding of biological macromolecules and its associated dynamics are critical to our understanding of life.^[1] Unfortunately, most ways of studying these processes such as thermal and chemical denaturation are not reversible and experiments must be designed to track time dependent structural changes as the macromolecule transitions from the initial

^{a)} maugust@ucdavis.edu.

native folded state to the final denatured, unfolded state and vice-versa.^[2–3] Prompted by early nuclear magnetic resonance (NMR) work on liquids by Jonas and coworkers^[4,5] at extreme pressures, Wand and coworkers^[6] pioneered the application of multidimensional high resolution liquid state NMR spectroscopy to the characterization of ambient condition folded macromolecules and their unfolded counterparts at moderate applied pressure, P, and room temperature. That work took advantage of the fact that pressure induced unfolding is reversible. Indeed, Wand and coworkers demonstrated this fact with several examples wherein the high pressure NMR parameters returned to their ambient values when the pressure was removed.^[6] These early experiments compared NMR derived structures obtained at ambient conditions to high pressure ($P < 2$ kbar) structures and most likely did not consider the dynamics of the structural transition because the NMR pressure hardware did not exist.

The rich history of fast temperature ramping or T-jump experiments in biological folding problems is not similarly enjoyed by the high pressure community. For example, the commercially available Daedalus syringe pump based systems designed to interface with most NMR spectrometers can at best change the sample pressure by 2 kbar in 1 minute, yielding $dP/dt = 33$ bar/s. This pressurization rate is too slow to study folding dynamics.

Recently, Bax and coworkers^[7] developed a syringe pump system capable of dropping the pressure of a room temperature NMR sample from 2 kbar to ambient conditions in 2 ms. The significantly improved depressurization rate of $dP/dt = -1$ Mbar/s is adequate to track protein folding with conventional high resolution multidimensional NMR spectroscopy, as elegantly demonstrated by Bax and coworkers in the folding of ubiquitin.^[7]

The work featured here uses high resolution, liquid state, one dimensional ^1H NMR spectroscopy along with a commercially available Daedalus syringe pump system to experimentally estimate the temperature change in water T_w due to compression heating and decompression cooling inherent in the fast P-jump experiments by Bax and coworkers mentioned above.^[7] Measured data for the specific volume $V(T,P)$, the coefficient of thermal expansion $\alpha(T,P)$, and the heat capacity $C_p(T,P)$ of water can be used to describe the temperature T as a function of the pressure P for an adiabatic process as^[8]

$$\frac{dT}{dP} = \frac{V(T,P)\alpha(T,P)}{C_p(T,P)}T. \quad (1)$$

An iterative numerical solution to this equation yields the solid line shown in Fig. 1 that provides the expected temperature change T_w values following application of the abscissa pressure to 298 K, 1 bar ambient condition water. The cross “+” and “x” symbols in Fig. 1, respectively correspond to T_w values calculated from Eq. 1 neglecting the T and P dependence of $V(T,P)$, $\alpha(T,P)$, and $C_p(T,P)$. The T_w value, indicated by the cross symbol, uses the ambient condition values for these parameters while the T_w value, indicated by the “x” symbol, uses room temperature and $P = 2$ kbar values for these parameters. Bax and coworkers estimated the temperature change during P-jump experiments using the former approach and arrived at a similar number^[7], slightly smaller than the exact value described by the solid line in Fig. 1.

Unfortunately, the change in the ^1H chemical shift of pure water is not known as a function of pressure, and since most aqueous solutes have similar unknown pressure dependent chemical shifts, it is nearly impossible to study water directly. Ethylene glycol, on the other hand, is an ideal candidate for this study as the methylene and hydroxyl protons are two sets of chemically inequivalent nuclei that yield two distinct chemical shifts.^[9] Moreover, it is known that the chemical shift of the hydroxyl proton is temperature dependent, reflecting an equilibrium between cis and trans hydroxyl proton configurations. It is this fact that Van Geet used in the development of ethylene glycol as a ^1H chemical shift based NMR temperature standard.^[10] As the chemical shift difference between the methylene and hydroxyl ^1H peaks σ is temperature dependent and reflects chemical equilibrium, it stands to reason that σ will also depend on pressure. Once the equilibrium values of $\sigma(T,P)$ as a function of T and P are measured, instantaneous values of T can be calculated from knowledge of P during pressurization and measured $\sigma(T,P)$ values. The calculated temperatures before and after pressurization are used to define a measured temperature T_{meas} that, when corrected to account for heat loss, yields a temperature change for ethylene glycol T_{eg} that can be compared to theoretical predictions in Fig. 1 for the temperature change in water T_{w} .

2.0 Materials and Methods

Ethylene glycol (99.93 %) samples were used as received from Fisher Scientific. A Daedalus Innovations Xtreme-60 Syringe Pump in conjunction with a Daedalus Innovations zirconia 2 kbar rated 640 μL NMR cell, were used to pressurize samples. To prevent the dissolution of the ethylene glycol sample into the pressure transmission fluid water, a small $\approx 40 \mu\text{L}$ volume of heavy paraffin oil obtained from Fisher Scientific was floated on top of the sample to form a gasket. Small sample NMR measurements were accomplished using an Oxford Instruments 6.95 T superconducting solenoid magnet, a Tecmag Apollo NMR spectrometer and a commercial GE 300 MHz liquid state NMR probe. Custom made Teflon spacers were used to interface the probe to the NMR cell. A Love Controls series 16A temperature controller and K-type thermocouple were used to heat and maintain sample temperatures when needed.

The room temperature T_0 pressure dependence of the ethylene glycol methylene/hydroxyl ^1H chemical shift difference $\sigma(T_0,P)$ was obtained from ^1H NMR spectra recorded in 20 bar increments in the $0 \text{ bar} < P < 2,000 \text{ bar}$ range. Note that 0 bar represents gauge pressure and is equivalent to atmospheric pressure. After the desired pressure was established, the sample was allowed to equilibrate for 10 minutes to room temperature and a single scan, one radio frequency (rf) pulse NMR spectrum was recorded. This process was repeated over the desired pressure range.

The full equilibrium $\sigma(T,P)$ surface was determined at multiple applied temperatures and pressures. Temperatures ranged from 293 K to 323 K in 5 K increments and applied pressures ranged from 0 bar to 2,000 bar in 250 bar increments. To establish these various sample conditions, the sample was first pressurized and allowed to equilibrate for 20 – 30 minutes at room temperature. The sample was then heated to the desired temperature and allowed to equilibrate another 20 – 30 minutes to ensure uniform sample heating. The single

scan, one rf pulse NMR spectrum was then recorded to obtain $\sigma(T,P)$ at the targeted T and P values.

Transient pressure σ values for ethylene glycol were recorded during pressurization of the sample. Here the single scan, one rf pulse NMR spectrum was used to obtain σ every 2 s during pressurization and data was recorded for one hour after the set pressure was established. The syringe pump began ramping to the set pressure 60 s after data acquisition started. In this way, transient shift differences σ were obtained before pressurization, during the pressure ramping period and during sample equilibration at room temperature and at the various set pressures of P = 500, 1,000, 1,500 and 2,000 bar.

3.0 Results

The plot shown in Fig. 2(a) is the ethylene glycol barometer analog of the ethylene glycol thermometer described in detail by Van Geet.^[10] Here the pressure is varied within the $0 < P < 2$ kbar range, the temperature is held constant at $T_0 = 298$ K and $\sigma(T_0,P)$ is recorded as described above. Measured data is reported as solid gray circles while the black solid line corresponds to a linear fit function with $R^2 = 0.99$. The $\sigma(T_0,P) = 1.69 \text{ ppm} + (4.35 \times 10^{-5} \text{ ppm/bar}) P$ fit function can be extended to much higher pressure and used to verify the pressure established in a clamp – cell NMR probe as shown in Fig. 2(b). The design, construction and use of the clamp – cell NMR probe is described elsewhere.^[11] The “x” symbols in Fig. 2(b) corresponds to ethylene glycol $\sigma(T_0,P)$ values obtained at P = 0 and 10 kbar using the clamp – cell NMR probe.

Varying both temperature and pressure leads to the measured $\sigma(T,P)$ ethylene glycol values shown as points in Fig. 3. The mesh surface in Fig. 3 represents the function

$$\Delta\sigma(T, P) = \sum_{n,m=0}^2 \sigma_{n,m} (T - T_0)^n (P - P_0)^m \quad (2)$$

with $T_0 = 298$ K, $P_0 = 0$ atm, and the best fit, second order surface polynomial with 95% confidence bounds, $\sigma_{n,m}$, listed in Table 1.

The data shown in Figs. 2 and 3 correspond to equilibrium conditions at specified T and P values. The σ values shown in Fig. 4(a) were recorded in real time as the syringe pump increases the pressure from 0 to a constant 1.5 kbar in 60 s as shown in Fig. 4(b). Solving Eq. 2 for T using the measured σ values in Fig. 4(a) and the $\sigma_{n,m}$ values in Table 1 yields the calculated temperature behavior shown in Fig. 4(c). The temperature difference T_{meas} shown in Fig. 4(c) is reported at selected pressures in Table 2.

4.0 Discussion

The variation of σ as a function of temperature at atmospheric pressure is central to the operation of the ethylene glycol NMR thermometer. As originally shown in the pioneering work of Van Geet, the sign of $d\sigma/dT|_P$ is negative, implying that σ decreases in value as the temperature is increased.^[10] The opposite trend is observed with increasing pressure at room temperature in Fig. 2. In this case, the sign of $d\sigma/dP|_T$ is positive, implying that σ

increases as the pressure is increased. The room temperature increase in σ appears to be a linear function of pressure up to 10 kbar as shown in Fig. 2(b). The σ values as a function of pressure in Fig. 2(a) were used to calculate the slope and intercept of the best fit solid line. The solid line shown in Fig. 2(b) is an extension of this best fit line, a line that agrees quite well with measurements from two different NMR probes.

Access to both the Daedalus equipment and a homebuilt variable temperature NMR probe insert allowed determination of $\sigma(T,P)$ equilibrium values in the $0 < P < 2$ kbar and $293 < T < 323$ K ranges as shown in Fig. 3. Note that the T and P axes in this plot increase from right to left. As expected on the basis of Van Geet's work at room pressure, the sign of $d\sigma/dT|_P$ is negative up to the maximum 2 kbar pressure studied. Similarly, as expected from Fig. 2, the sign of $d\sigma/dP|_T$ remains positive up to the maximum 323 K temperature studied. These observations are reinforced by the respective values of $\sigma_{1,0}$ and $\sigma_{0,1}$ provided in Table 1 for the best fit of the data shown as dots in Fig. 3 to Eq. 2, which is represented as the wire mesh in Fig. 3.

The fact that the signs of $d\sigma/dT|_P = \sigma_{1,0}$ and $d\sigma/dP|_T = \sigma_{0,1}$ are different is important for two reasons. The first is chemical. The fact that $\sigma(T,P)$ changes at all with pressure and temperature suggests at least a two state chemical equilibrium process that can be described by an isomerization reaction. Taking the reactants to be cis ethylene glycol with hydroxyls on the same side of the molecule, and the products to be trans ethylene glycol with hydroxyls on opposite sides of the molecule, permits some interesting thermodynamic commentary. One would expect the cis \rightarrow trans transformation to be exothermic because the trans configuration is sterically stable. As the cis conformation is more sterically hindered, there will be a release of potential energy upon conversion to the trans conformation. As the temperature is increased at room pressure according to Van Geet's work, LeChatelier's principle dictates that the reaction will shift at equilibrium to produce the cis conformation and a chemical shift closer to the methylene resonance in the ^1H NMR spectrum of ethylene glycol. Previous variable pressure NMR work on small molecules and biological macromolecules indicates that molecules unfold with increased pressure to accommodate more water molecules into their hydration sphere.^[12-13] In the case of ethylene glycol, this means that the trans conformation is favored at high pressure and a chemical shift further from the methylene resonance in the ^1H NMR spectrum of ethylene glycol is displayed. This arguably primitive thermodynamic analysis suggests that the combination of high pressure and low temperature will generate the trans conformation while low pressure and high temperature will produce the cis conformation.

It is the size difference between $\sigma_{1,0}(T - T_0)$ and $\sigma_{0,1}(P - P_0)$ in ethylene glycol that allows any measured change in $\sigma(T,P)$ to be observed during compression heating or decompression cooling. In the relevant temperature and pressure range where the signs of $\sigma_{1,0}$ and $\sigma_{0,1}$ are different, it is clear that increased pressure and temperature competitively impact the observed $\sigma(T,P)$ value. The greater the size difference between $\sigma_{1,0}$ and $\sigma_{0,1}$, the greater the $\sigma(T,P)$ value, and the greater the sensitivity to changes in temperature and pressure.

Fortunately, the size difference between $\sigma_{1,0}$ and $\sigma_{0,1}$ for ethylene glycol is large enough in the temperature and pressure ranges relevant to compression heating and decompression

cooling that a measurement is possible. The data shown in Fig. 4(a) describes the behavior of σ when the applied pressure is quickly jumped from 0 to 1.5 kbar as shown in Fig. 4(b). Before the pressure is increased, σ remains constant. As the applied pressure is linearly increased according to Fig. 4(b), the σ value increases, reflecting the fact that $|\sigma_{0,1}(P - P_0)| > |\sigma_{1,0}(T - T_0)|$. As soon as the final maximum applied pressure is established, heating ceases and the sample begins to cool. Since the sign of $\sigma_{1,0}$ is negative, a drop in temperature at fixed pressure corresponds to an increase in $\sigma(T,P)$ value, consistent with Fig. 4(a).

In the limit that the cis \rightarrow trans equilibrium is established on a time scale much faster than is detectable by NMR spectroscopy, the transient σ values shown in Fig. 4(a) can be used with the applied pressure in Fig. 4(b) and the parameters in Table 1 to calculate an “instantaneous” temperature by solving Eq. 2 for T. The calculated temperature for the 1.5 kbar pressure jump in Fig. 4(b) is shown in Fig. 4(c). As expected, and shown in Fig. 4(c), sample compression causes sample heating during the $t_{\text{obs}} = 60$ s pressurization period. Moreover, after the pressurization is complete, the sample begins to cool to room temperature. The time constant for the temperature return to ambient conditions is $t_{\text{loss}} = 233$ s from Fig. 4(c). This value is independent of the pressure jump size and is a complex function of the heat exchange between the macroscopic ethylene glycol and the surroundings, through the zirconia cell, the wax gasket, and the pressure transmission fluid, water. Of interest here is the temperature change during sample pressurization T_{meas} as shown in Fig. 4(c). A summary of T_{meas} values is provided in Table 2.

While the trend in T_{meas} values shown in Table 2 is sensible, the magnitude of these values is inconsistent with a theoretical estimate. Greater pressure changes translate into larger temperature jumps, here, $T_{\text{meas}} = 1.47$ and 5.33 K at applied pressure jumps of $P = 500$ bar and 2,000 bar respectively. Unfortunately, the following estimate of T_{meas} for ethylene glycol suggests that these experimental values are too small. The solid line in Fig. 1 can be used to find $T_w = 2.73$ K for water upon a 2 kbar compression. Careful work in the food processing industry determined the ratio of the isothermal compressibility to the coefficient of thermal expansion $dT/dP|_V$ for ethylene glycol and water at ambient conditions.^[14] The ratio of these values, $\xi = (dT/dP|_V)_{\text{eg}} / (dT/dP|_V)_w = 2.8636$, can be used to estimate the expected temperature change for ethylene glycol as $T_{\text{eg}} = \xi T_w = 7.82$ K. This estimated number is ca. 2 K or 20 % greater than the measured number for ethylene glycol reported in Table 2. The likely reason for this discrepancy is that this estimate presumes a thermally isolated system. According to the cooling trend shown in Fig. 4(c) at long time this is not the case. The time constants for compression heating t_{obs} and thermal cooling to the surroundings at pressure identified above t_{loss} can be used to define a correction factor $\eta = 1 - t_{\text{obs}}/t_{\text{loss}} = 0.74$ that scales the expected theoretical maximum temperature change for ethylene glycol to the measured temperature change as $T_{\text{meas}} = \eta T_{\text{eg}}$. Application of this scaling factor to the expected $T_{\text{eg}} = 7.82$ K value yields 5.78 K, a temperature difference close to the $T_{\text{meas}} = 5.33$ K value observed upon 2,000 bar compression. The values reported in the column labelled as T_{eg} in Table 2 were obtained by reversing this relation to estimate the theoretical maximum T_{eg} value from T_{meas} . A similar inverse relation uses the ξ ratio to infer T_w from T_{eg} and these values are also provided in Table 2. At 2,000

bar, the inferred $T_w = 2.50$ K value obtained in this way compares well with the 2.73 K theoretical value.

An interesting aspect of this work is that despite all NMR measurements being accomplished on pure ethylene glycol, pure water temperature change data with pressure is inferred using thermodynamic parameters from the food processing community. All inferred T_w values corresponding to the applied pressure changes shown in Table 2 are consistent with theoretical estimates. The T_w values in Table 2 are reproduced as the open circles in Fig. 1. The agreement between theory shown as the solid line in Fig. 1 and the experimental NMR derived values is remarkable.

The purpose of this work was to experimentally determine whether or not rapid sample compression or decompression causes temperature changes that could interfere with pressure induced protein folding dynamics. Characterization of the temperature and pressure dependent chemical shift of ethylene glycol was used to infer a temperature change for water in order to verify theoretical predictions as shown in Fig. 1. Although the expected temperature change estimated by Bax and coworkers^[7] using ambient condition thermodynamic parameters is low, as shown by the cross in Fig. 1, it is only ca. 0.6 K lower than the true value. A slightly better high pressure estimate shown by the “x” is based on room temperature, elevated pressure thermodynamic parameters. Regardless of the approximation method, the overall change for temperature change for water is theoretically and now experimentally predicted to be ca. 2.7 K for a 2 kbar compression/decompression, a temperature change that should not interfere with rapid pressure jump protein folding studies.

5.0 Conclusion

¹H NMR measurements on ethylene glycol reveals that σ is both temperature and pressure dependent. The difference in sign of the temperature and pressure dependent σ slopes suggests that the cis \rightarrow trans ethylene glycol equilibrium is exothermic. The equilibrium $\sigma(T,P)$ surface was used along with instantaneous σ values and known pressure to calculate a temperature. This T_{meas} was corrected for heat loss to the surroundings during compression and an experimental value for the temperature rise of water was inferred. These inferred temperatures were consistent with theoretical predictions. This works arms structural biologists with information that confirms that the temperature rise in water associated with compression heating and decompression cooling is insignificant in the study of protein folding problems with P-jump NMR.

Acknowledgements

Support of this work from the California League of Food Processors, the Center for Process Analysis and Control, and the National Institutes of Health through Grant No. R01 EY012347 is gratefully acknowledged.

References

- [1]. Anfinsen CB, Biochem. J 1972, 128, 737. [PubMed: 4565129]
- [2]. Akasaka K, Yamaguchi T, Yamada H, Kamatari Y, Konno T, NMR approaches to the heat-, cold-, and pressure-induced unfolding of proteins, Oxford University Press 1997, 157.

- [3]. Goetz J, Koehler P, LWT-Food Sci. Techno 2005, 38, 501.
- [4]. Nash DP, Jonas J, J. Biochem. Biophys. Res. Commun 1997, 238, 289. [PubMed: 9299496]
- [5]. Samarasinghe SD, Campbell DM, Jonas A, Jonas J, Biochemistry 1992, 31, 7773. [PubMed: 1510963]
- [6]. Kranz JK, Flynn PF, Fuentes EJ, Wand AJ, Biochemistry 2002, 41, 2599. [PubMed: 11851407]
- [7]. Alderson TR, Charlier C, Torchia DA, Anfinrud P, Bax A, J. Am. Chem. Soc 2017, 139, 11036. [PubMed: 28766333]
- [8]. Ter Minassian L, Pruzan P, Soulard A, J. Chem. Phys 1981, 75, 3064.
- [9]. Kaplan ML, Bovey FA, Cheng HN, Anal. Chem 1975, 47, 1703.
- [10]. Van Geet AL, Anal. Chem 1968, 40, 2227.
- [11]. Augustine MP, Ochoa G, Casey WH, Am. J. Sci 2017, 317, 846.
- [12]. Helm L, Merbach AE, Coord. Chem. Rev 1999, 187, 151.
- [13]. Pisaniello DL, Helm L, Meier P, Merbach AE, J. Am. Chem. Soc 1983, 105, 4528.
- [14]. Guignon B, Aparicio C, Sanz PD, J. Chem. Eng. Data 2010, 55, 3017.

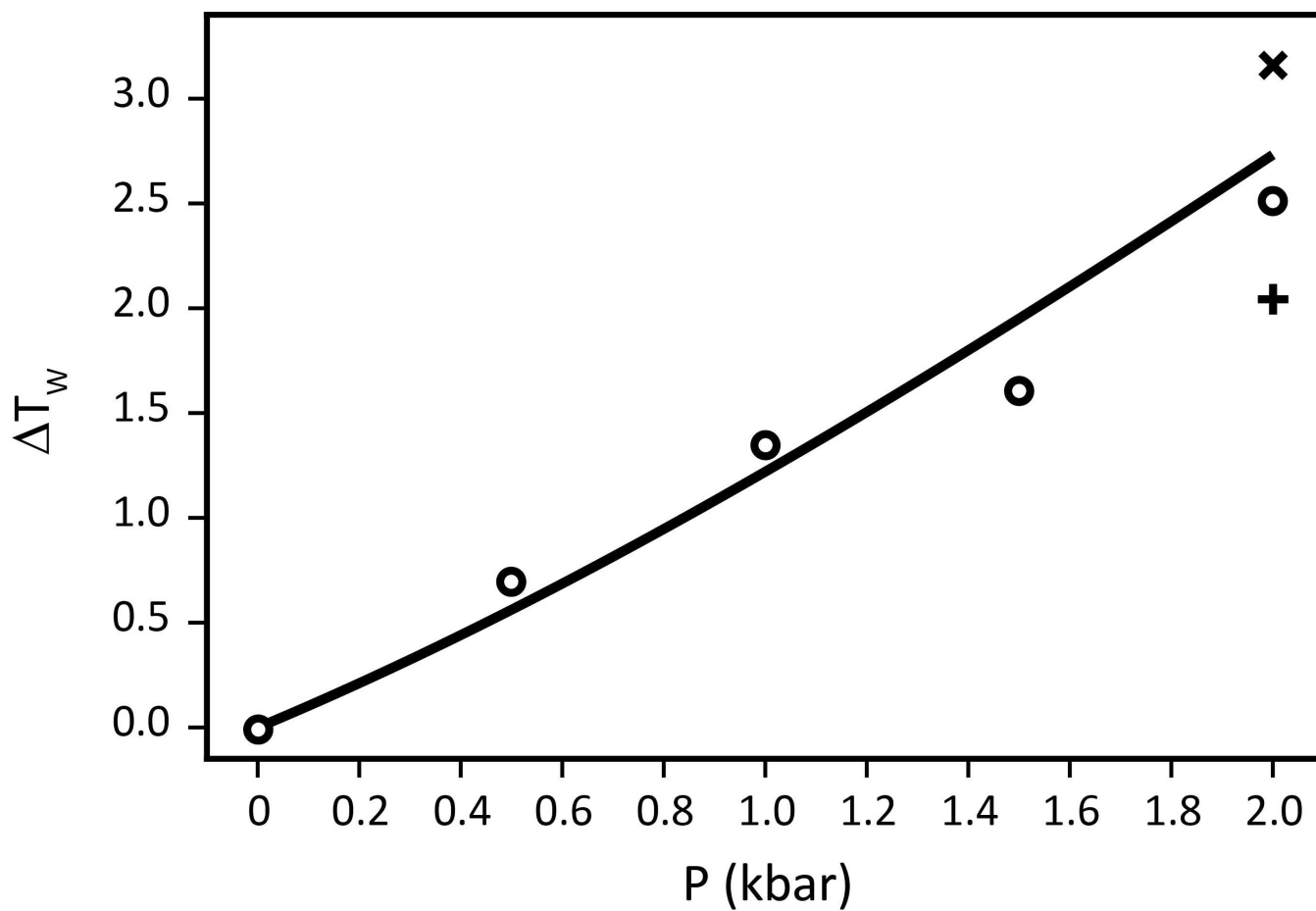


Figure 1.

The solid line corresponds to the solution to Eq. 1 using all available thermodynamic parameters for pure water. This line describes the expected temperature rise in water T_w due to an applied pressure change P . The “+” and “x” symbols are estimates using thermodynamic parameters respectively measured at room conditions and at elevated pressure and room temperature. The open circles are experimentally inferred values for water.

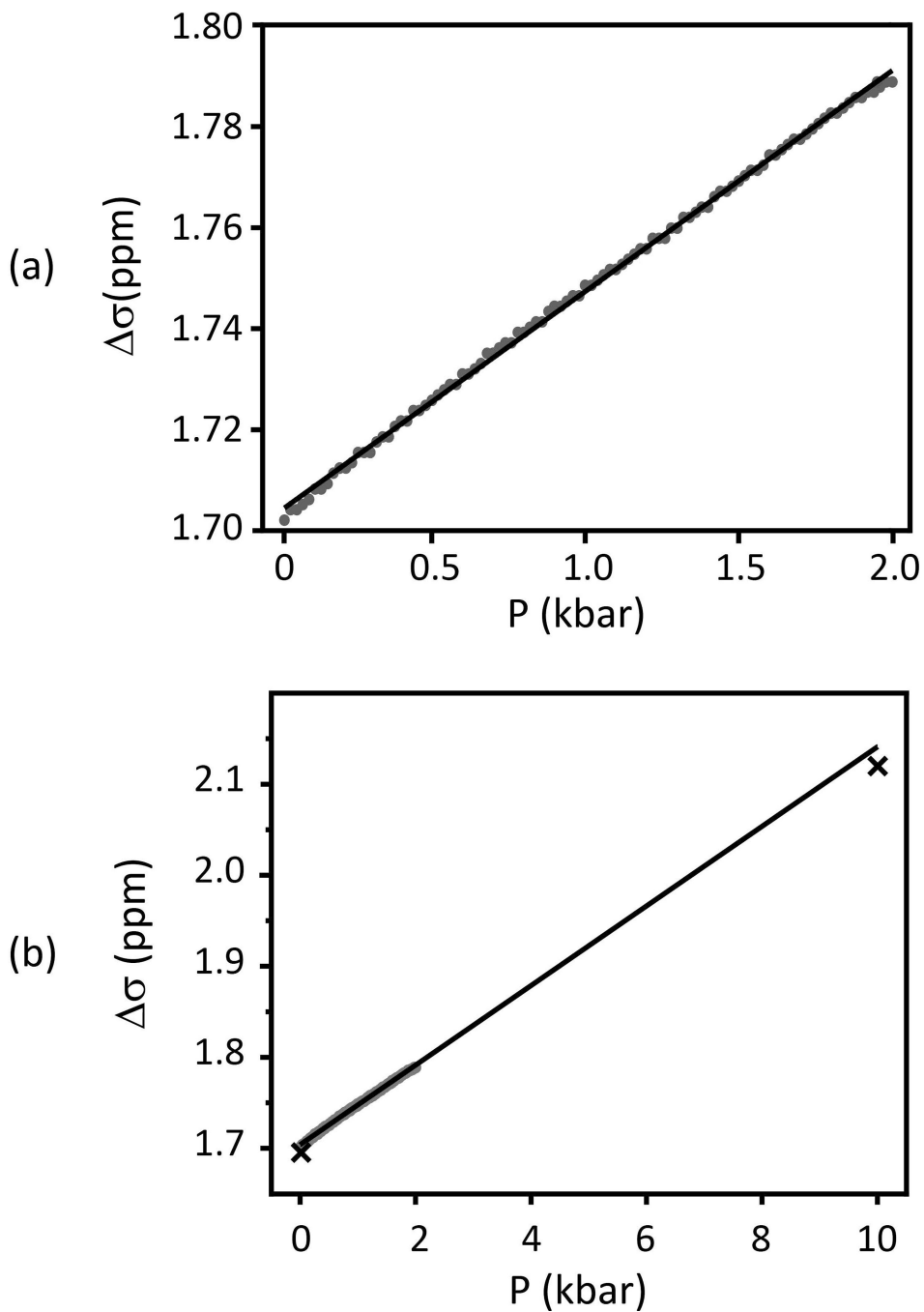


Figure 2. The solid gray circles correspond to measured $\Delta\sigma$ values for ethylene glycol at room temperature and the indicated pressure. The solid line shown in (a) represents a linear fit to the data. The “x” symbols in (b) correspond to $\Delta\sigma$ values obtained from a room temperature, clamp cell, high pressure NMR probe and the solid line is an extension of the linear fit line in (a). The low pressure $\Delta\sigma$ values are reproduced in (b) as a reference.

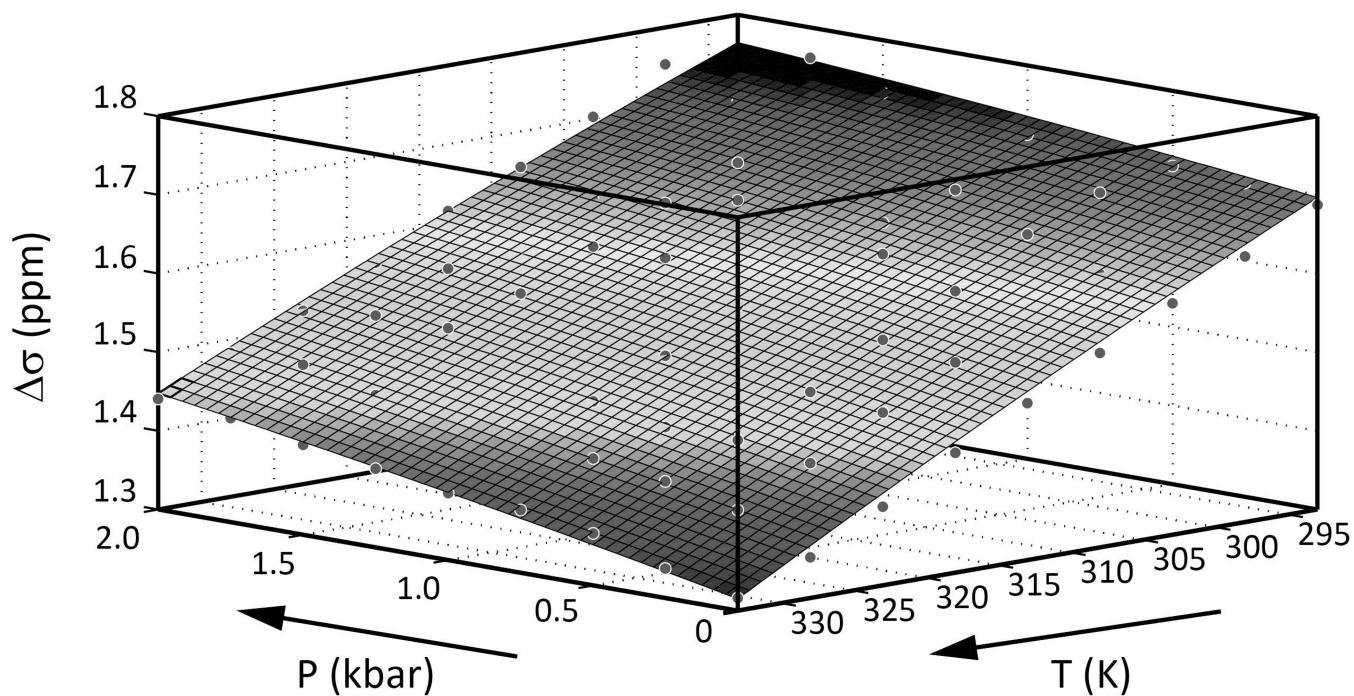


Figure 3. Measured equilibrium $\sigma(T,P)$ values shown as dots as a function of applied pressure and temperature. The wire mesh surface corresponds to Eq. 2 with values from Table 1. Note that both temperature and pressure increase from right to left.

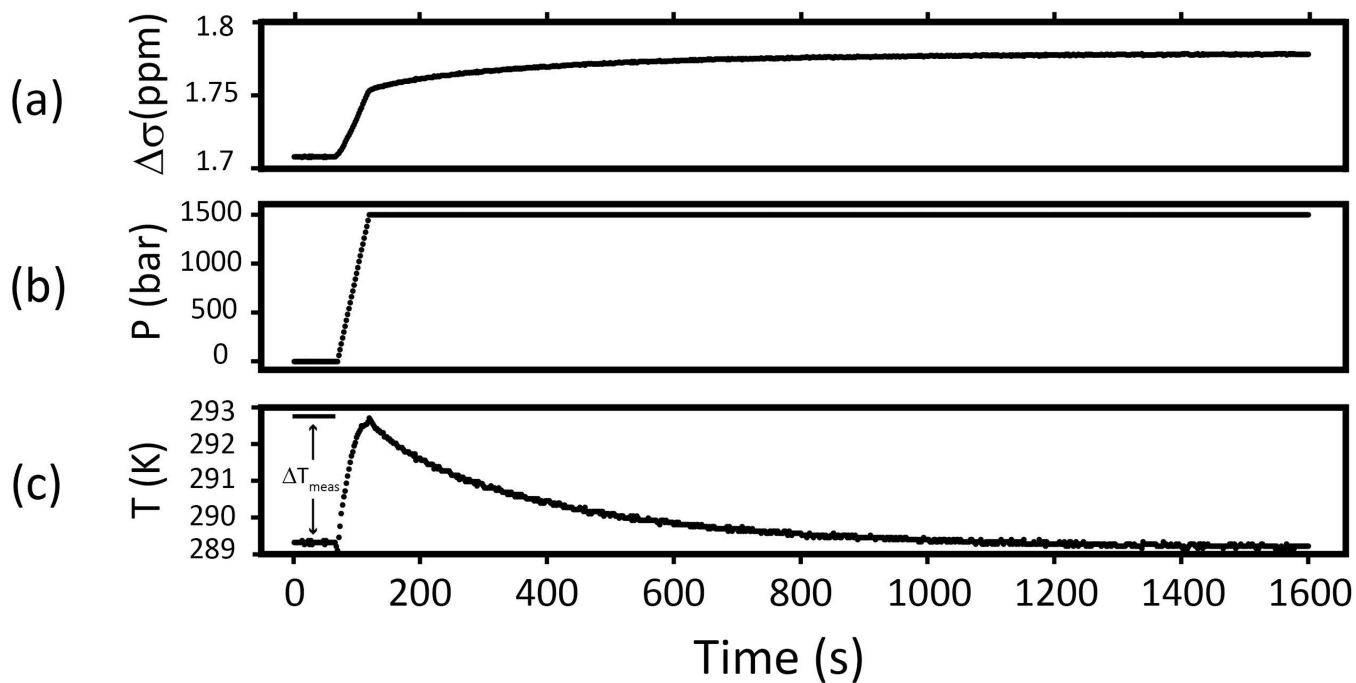


Figure 4.

Measured σ values for ethylene glycol in (a) as a function of the applied pressure shown in (b). Solving Eq. 2 for the temperature using the parameters in Table 1, the applied pressure in (b) and the measured σ in (a) results in (c). The T_{meas} shown in (c) is reported at four different maximum applied pressures in Table 2.

Table 1.Parameters obtained from fitting equilibrium $\sigma(T,P)$ data to Eq. 2.

n	m	$\sigma_{n,m}$	error
0	0	1.69 ppm	± 0.01 ppm
0	1	6.23×10^{-5} ppm/bar	$\pm 2.16 \times 10^{-5}$ ppm/bar
1	0	-7.92×10^{-3} ppm/K	$\pm 1.11 \times 10^{-3}$ ppm/K
1	1	5.13×10^{-7} ppm/(bar-K)	$\pm 4.27 \times 10^{-7}$ ppm/(bar-K)
0	2	-9.87×10^{-9} ppm/bar ²	$\pm 2.52 \times 10^{-9}$ ppm/bar ²
2	0	-2.83×10^{-5} ppm/K ²	$\pm 2.46 \times 10^{-5}$ ppm/K ²

Author Manuscript

Author Manuscript

Author Manuscript

Author Manuscript

Table 2.

Calculated and observed compression heating in ethylene glycol

P(kbar)	T_{meas}(K)	T_{eg}(K)	T_w(K)
0.5	1.47	1.98	0.69
1.0	2.86	3.86	1.34
1.5	3.40	4.59	1.60
2.0	5.33	7.16	2.50

Author Manuscript

Author Manuscript

Author Manuscript

Author Manuscript